

Microwave imaging based breast tumor detection using compact wide slotted UWB patch antenna

MD. TARIKUL ISLAM^{a,*}, M. SAMSUZZAMAN^b, M. R. I. FARUQUE^c, MANDEEP JIT SINGH^d, M. T. ISLAM^e
^{a,b,d,e}Center of Advanced Electronic and Communication Engineering, Faculty of Engineering and Built Environment
^cSpace Science Center (ANGKASA), Universiti Kebangsaan Malaysia, Malaysia

A compact ultra-wideband(UWB) antenna and an antenna array based Microwave Imaging system are presented in this paper. The presented antenna is consist of a rectangular slotted patch, tapered slot ground with 1.6 mm height which has a compact size of 21.44 × 23.53 mm². Numerous parameters are considered and optimized for using the proposed antenna in breast imaging system over ultra-wideband (UWB) frequency (3.1-10.6 GHz). The antenna offers an operating bandwidth of about 8.51 GHz (3.49-12 GHz) for reflection co-efficient -10dB with good impedance matching, 5.76 dBi of highest gain and about 92% of average radiation efficiency with stable radiation pattern. The fidelity factor is 82% for face to face direction and for side by side is 90%, that indicates the directionality and lower alteration of the received signal. The antenna is fabricated and the properties are measured to observe the antenna performance. The array setup of 7 antennas is used to measure the backscattering signal of the breast phantom and observe the significant change of signal with and without tumor cell inside the phantom. The images generated form the analysis of backscattering signal is presented.

(Received June 25, 2018; accepted August 20, 2019)

Keywords: Ultra wideband, Slotted patch, Microwave imaging, Breast imaging

1. Introduction

Microwave imaging has concerned significant research interest in the field of breast tumor detection. Microwave Imaging has important advantages over the existing conventional techniques for detecting breast tumor. Conventional systems are X-ray mammography, Magnetic Resonance Imaging (MRI) and Ultrasound Imaging. But it is a matter of safety due to the ionizing nature of existing systems. Although the procedure of existing systems are uncomfortable and painful for the patient and have the risk of false alarm. Though, ultrasounds offer only additional information with a low sensitivity for young patients[1], while MRI is an expensive way for screening.

Nowadays ultra-wideband (UWB) technology is a good candidate for microwave imaging application for its high data resolution, low complexity, high gain, lightweight and low profile. The antenna has to be electronically compact by not effecting the performance. High gain, linear phase variation, stable radiation pattern, low profile is the requirement for ultra-wideband applications. To design a compact, high-efficiency ultra-wideband antenna is still a challenge to the researchers.

Microwave-based medical imaging systems have been widely demoralized throughout the last few years especially ultra wideband (UWB) imaging as an alternative method to the existing imaging techniques. Comparing to existing X-rays, MRI and Ultrasound Imaging, microwaves are non-ionizing which allow regular investigations without any radiation risk. Besides, microwave imaging technology is comparatively low cost

and reliable comparing to existing conventional medical imaging technologies [2, 3].

Researchers working on the early detection of breast tumor since last few years [4-8]. The existing X-ray mammography has a high false alarm rate and some of the drawbacks including high radiation risk and uncomfortable breast compression during examination [9]. The limitations of existing systems lead the researchers to think of an alternative solution for breast tumor detection where microwave imaging is the good candidate in this field. Microwave imaging works on the basis of the variation in the dielectric properties of normal tissue and malicious tissue.

In terms of a breast tumor, there is a significant difference between the dielectric properties of regular breast tissue and a tumor cell. The dielectric properties of malignant breast tumor are higher than the normal breast tissue which is a key factor for using the microwave as breast imaging for finding tumor cells [10]. The investigated results of microwave imaging show the efficiency of microwave imaging techniques [8, 11-13]. Several UWB antennas are reported in [14-17].

The main working principle of microwave imaging is to transmit microwave signals across the target and receive the scattered signals in various directions. Because of having different dielectric properties of the different tissue the received scattered signal provides important information about signal propagation across the cells. Working on the received signals and by applying different algorithms it can be mapped the microwave image of the target. To design a reliable low-cost imaging system is the main aim of microwave imaging that can be simply applied for medical purposes. UWB antennas play a

significant role in efficient and effective imaging systems. The following characteristics should be fulfilled for using UWB antennas in microwave imaging applications:

- (1) the efficiency of directional power transmission into the target.
- (2) should be integrated to form an antenna array.
- (3) should be able to transmit and receive signals in a wide-ranging frequency,
- (4) should create good penetration into breast tissues.

In this paper, an UWB antenna with a dimension of only $21.44 \times 23.53 \text{ mm}^2$ was presented where the antenna was further used in microwave imaging of breast tumor. The antenna is compact in size comparing the antennas reported in [7, 18, 19]. The proposed antenna achieves an operating bandwidth of 3.49 to 12 GHz. The antenna performance of is observed experimentally and simulation. An antenna array is designed for the experiment of the behavior of the proposed antenna for Microwave Imaging. The proposed antenna shows an excellent performance in microwave imaging placing surrounding a breast phantom

including tumor cell. The observation results are presented in this article.

2. Antenna design and optimization

The main reason for choosing planner patch antenna for its simplicity, stable radiation pattern and compact low profile which can be used in several UWB applications as well as Microwave Imaging. The antenna design geometry and configuration are demonstrated in Fig. 1.

Typically, the bandwidth range of the patch antenna is not because of its multiple resonance part. A broad bandwidth can be acquired if it is possible to use multiple resonant parts where every part works frequently. The proposed microstrip antenna having a rectangular slotted radiating patch element along with a tapered shaped slot ground which is coupled to a 50-ohm microstrip-fed line. Different cuts ln , Wn , Wp are used for the modification of the patch to meet the desired bandwidth.

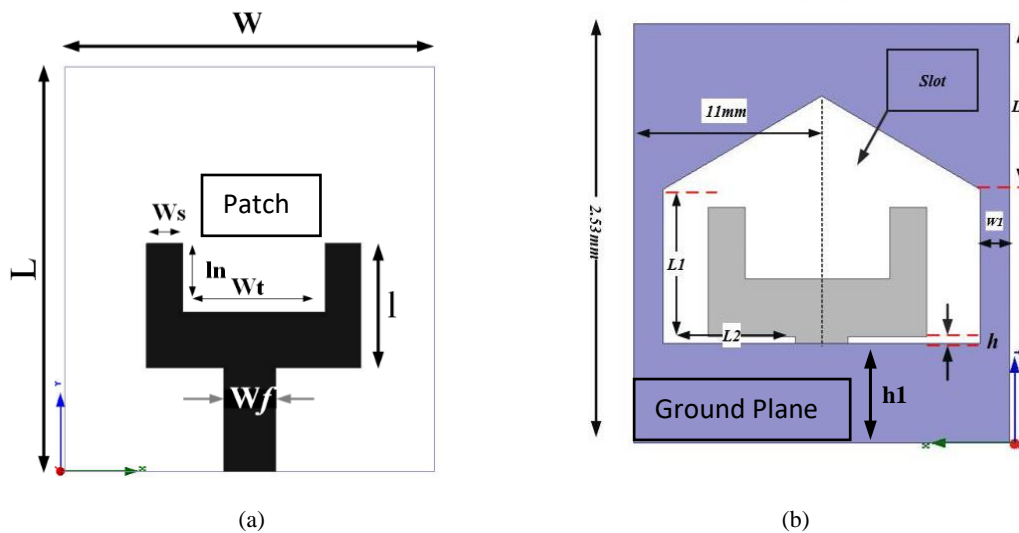


Fig. 1. The antenna geometry. (a) Top view, (b) Bottom view

Several patch shapes are tested while designing the proposed antenna. Fig. 2 displays the various tested patch shape including the proposed rectangular slotted patch. It is observed that by cutting a slot in rectangular patch and ground plane a high-frequency performance is achieved comparing to other a circular, elliptical, rectangular or square-shaped slot patch.

The reflection coefficient of the various patch shape is presented in Fig. 3 where the proposed patch shape acquires maximum bandwidth that helps to choose the proper patch shape for UWB applications. From the figure, it is identical that the proposed antenna achieves wide operating bandwidth with the proposed slotted tapered shaped patch. Fig. 4 shows the different ground shapes with proposed tapered one. Along with tapered slot ground, circular, elliptical and square slot ground with proposed slotted patch simulation results is observed. For choosing right ground slot shape, simulation with different shapes is

observed. Fig. 5 demonstrate the simulated reflection coefficient (S11) results with different ground structure with proposed one. It is observed that only for choosing tapered slot ground an UWB bandwidth is achieved. Fig. 6 shows the simulated s11 for different parameters of h1. By altering different values of $h1 = 4 \text{ mm}, 5 \text{ mm}, 5.5 \text{ mm},$ and $6 \text{ mm},$ at $h1=5.5 \text{ mm}$ the targeted bandwidth is acquired.

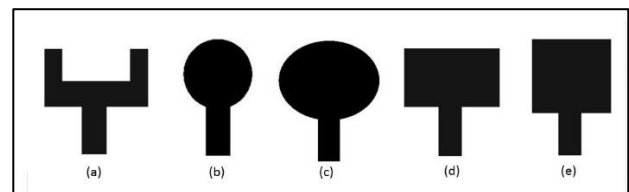


Fig. 2. Different tested patch shape: (a) rectangular slot (proposed) (b) circular slot (c) elliptical slot (d) rectangular and (e) square slot shape

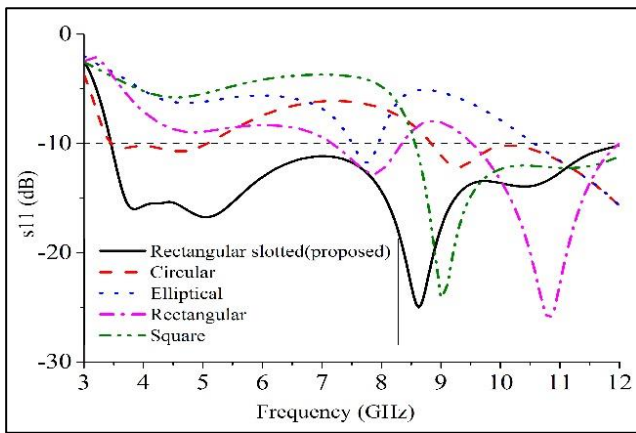


Fig. 3. Return loss (s_{11}) for different patch shapes

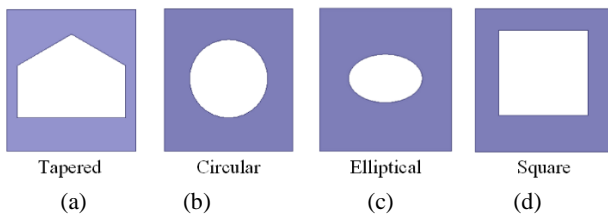


Fig. 4. Different tested ground shape: (a) Tapered (proposed), (b) Circular, (c) Elliptical and (d) Square slot

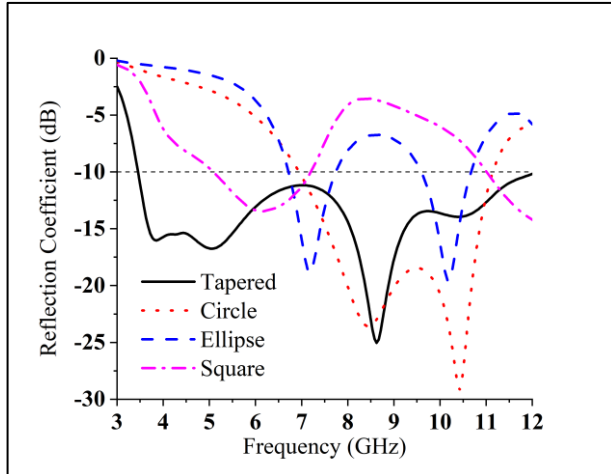


Fig. 5. Simulated S_{11} for different ground structure

By altering the value of l_n , w_p and w_n the antenna achieves wider bandwidth. The proposed antenna is fabricated on an inexpensive FR4 substrate. The relative permittivity of the substrate is 4.6 and loss tangent is 0.02. The tapered slot ground plane has a suitable matching with the microstrip transmission line. By proper patch shape selection and feeding techniques, a high performance of bandwidth, good gain and stable radiation pattern is achieved with only having the dimension of $21.44 \times 23.53 \text{ mm}^2$ which is very compact in size. Different adjusted

constraints of the proposed antenna are presented in Table 1.

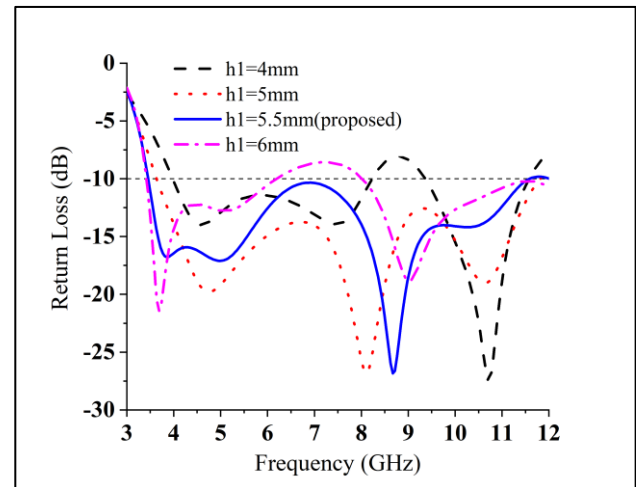


Fig. 6. Return loss (S_{11}) of different values of h_1

Table 1. Different adjusted parameters

Parameters	Value (mm)	Parameters	Value (mm)
W	21.44	L_3	9.30
L	23.53	W_t	8.244
W_s	2.11	l	7.24
L_n	4	h	1.6
L_1	8.66	W_p	1.98
L_2	7.52	W_f	3

3. Results and discussions

A. Frequency-domain performance

The proposed antenna has been simulated with the High-Frequency Structural Simulator (HFSS) and the Computer Simulation Technology (CST). After the fabrication of the antenna, the performance of the proposed antenna is investigated. At the beginning, different patch shape antennas are simulated to observe the UWB performance.

By increasing the coupling between the rectangular slot patch along with fed line by changing the slot shape and size decent impedance matching can be achieved. The fabricated picture of the antenna with top and bottom view is represented in Fig. 7(a) and 7(b) correspondingly. The fabricated antenna has been measured using the Satimo near Field Measurement Lab (UKM StarLab) using Satimo passive measurement (SPM) and SatEnv software and Agilent N5227A performance network analyzer. The measurement setup procedure is shown in Fig. 7(c) and 7(d).

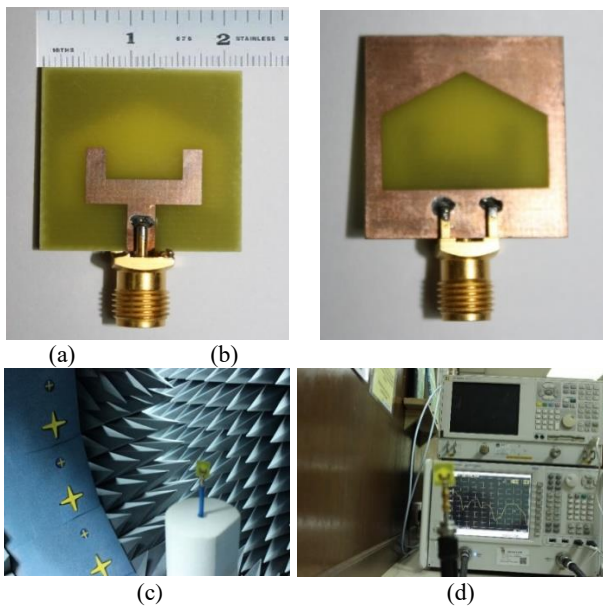


Fig. 7. Proposed antenna image after fabrication (a) Upper view, (b) Bottom view and measurement processes (c) and (d)

Fig. 8 illustrates the return loss (S_{11}) against frequency covers the entire bandwidth from 3.49 to 12 GHz with a return loss ≤ 10 dB range. This bandwidth is suitable for various UWB applications. Due to manufacturing tolerances and defective soldering of SMA connector a little disagreement between measured and simulated results is noticed. Fig. 9 shows in the proposed antenna's phase deviation of the input impedance. It shows almost linear phase variation across the operating bandwidth.

The linear phase variation regarding operating frequency specifies the same delay and pulse variation. Fig 10 shows the circulation of surface current for three different operating frequencies of 3.5GHz, 6.5GHz and 8.5 GHz. All the mentioned frequencies are shown in figure, feeding line carried out a large amount of current at the point of creation of electric. Comparing to a higher frequency the current distribution is steadier at a lower frequency because for higher frequency current flow become non-linear and the main current is conducting around the patch. Both the bands, the excitation is strong across the total portion of the antenna. For the higher frequency a large portion of current exists around the edge of cutting plane. Fig. 11 illustrates the simulated and tested antenna gain. It acquires an average gain of 4.2 dBi.

The simulated and measured efficiency is displayed in Fig. 12. It is observed that the antenna has a consistent and acceptable efficiency with a maximum of 96% at 7.25 GHz. The result is slightly varied because of feeding techniques and use of the low-cost FR4 substrate during measurement. Fig. 12a-c shows the measured and simulated 2D and 3D radiation patterns at two major planes explicitly, xz-plane and yz-planes for three frequencies of 3.5 GHz, 6.5 GHz, and 9.5 GHz. From Fig. 13(a), 13(b)

and 13(c), it is observed that with low cross-polarization, radiation patterns are omnidirectional in both the plane at a lower frequency of 3.5 GHz values. The same result is also observed from 3D radiation pattern. At a medium frequency of 6.5 GHz, the antenna radiates Omnidirectionally in both the plane. 2D and 3D measured and simulated radiation pattern shows a durable omnidirectional pattern across the surface. It is observed that in yz-plane the radiation pattern is omnidirectional but slightly directional in xz-plane at the higher frequency of 9.5 GHz. We notice a stable radiation pattern over the bandwidth.

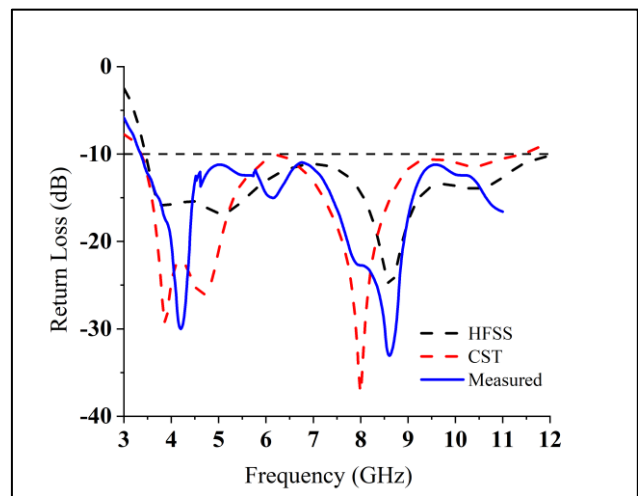


Fig. 8. Return loss (S_{11})

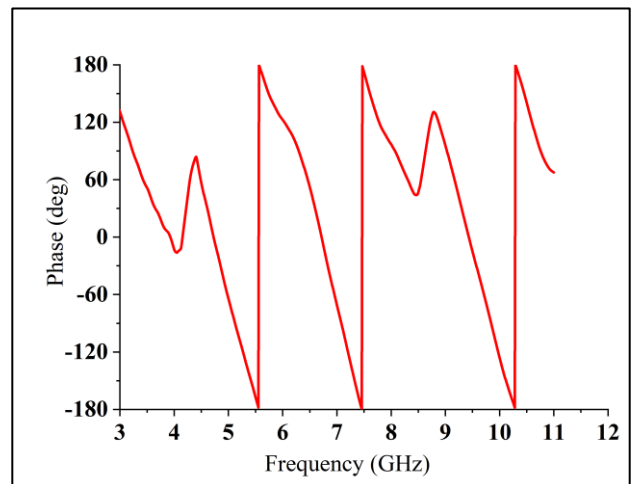


Fig. 9. Phase variation of the input impedance

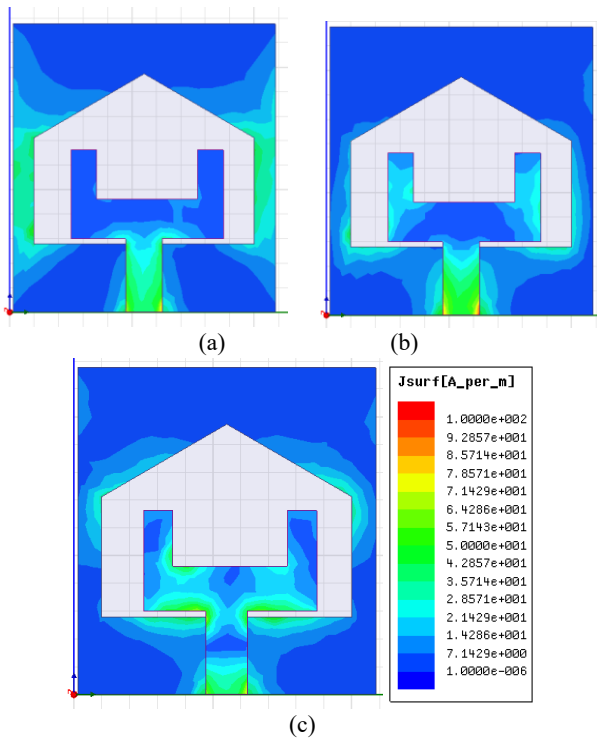


Fig. 10. Surface Current Distribution at (a) 3.5 GHz, (b) 6.5 GHz and (c) 9.5 GHz

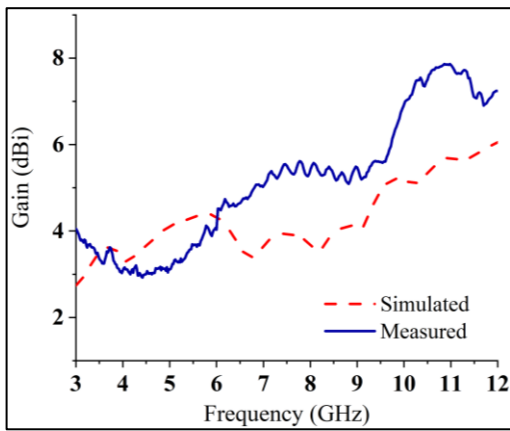


Fig. 11. Antenna Gain

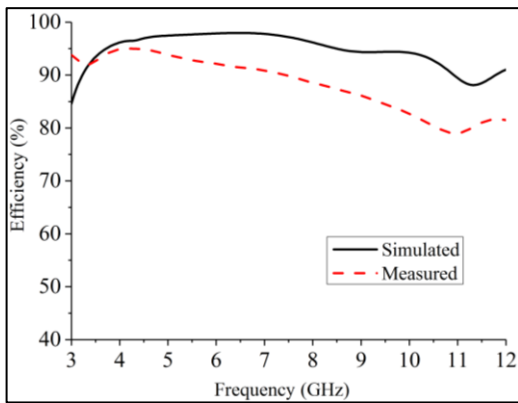


Fig. 12. Radiation Efficiency

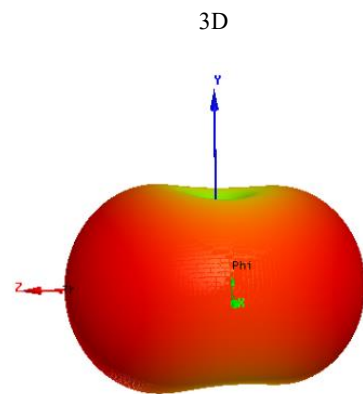
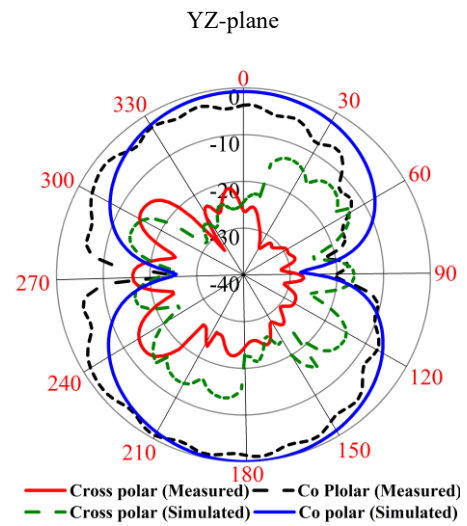
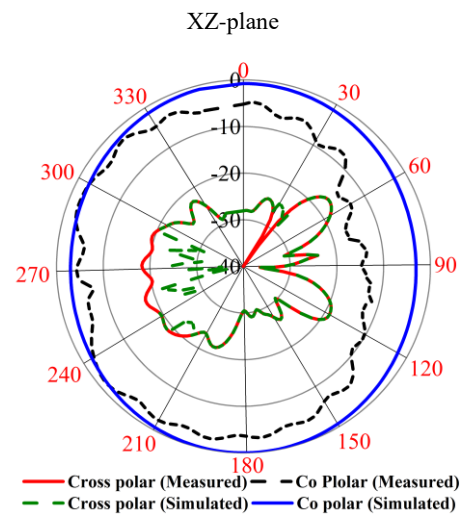


Fig. 13. (a) 2D and 3D Radiation Pattern at 3.5 GHz

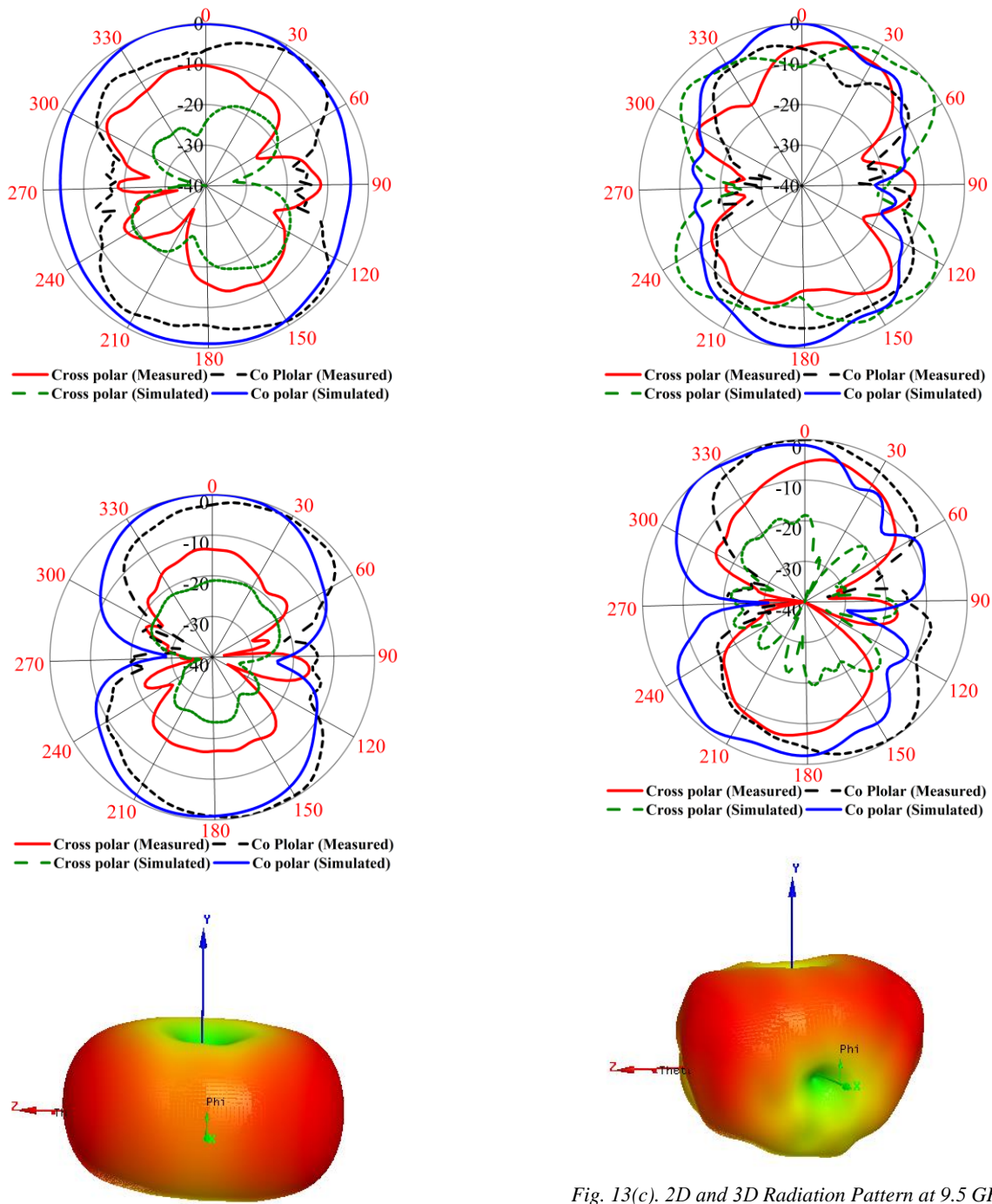


Fig. 13(b). 2D and 3D Radiation Pattern at 6.5 GHz

Fig. 13(c). 2D and 3D Radiation Pattern at 9.5 GHz

B. Time-domain performance

From the previous section, it is observed that the proposed antenna demonstrates excellent frequency-domain performance. Though, only decent frequency-domain characteristics cannot guarantee the antenna's sound behavior along with time domain. Thus, for the evaluation of the accuracy of the proposed antenna for microwave imaging systems, it is required to examine time-domain behavior which includes the transmission coefficient, input-output pulse waveform and group delay. Fig. 14 represents the transmission coefficient $|S_{21}|$ using two matching proposed antennas fronting each other and

side by side position which detached by a distance of 300mm, considering far field environs across whole UWB frequencies. The figure shows a flat magnitude of transmission coefficient line over the operating band. A slight reduction is observed at side by side scenario at the frequency of 10.1 GHz including flat magnitude over rest of the bandwidth which indicates stable UWB transmission ability in both faces to face and side by side case. The group delay is distinct as the first derivative of the far field phase of the transmission response regarding the radial frequency ω . Fig. 15 defines the measured group delay of the antenna in the face to face and side by side scenario. The observation shows two sharp variations of the group delay in the frequency bands at 4.5 and 8.5 GHz which specifies the slight unconventionality from linear phase response. The group delay remains almost constant at other frequencies outside the affected bands that show good phase linearity. The input and received signals in face-to-face and side-by-side orientation with the distance of 300 mm of the proposed antenna is shown in Fig. 16(a) and 16(b), individually. From the transmitting and receiving pulse, we observe that the received signals of both the orientations have parallel waveforms having a small variation.

A key factor is known as the fidelity factor (FF) [20] is also calculated to validate the correspondence between the transmitted (TX) and received (RX) signals.

$$F = \text{Max}_\tau \left| \frac{\int_{-\infty}^{+\infty} s(t)r(t-\tau) dt}{\sqrt{\int_{-\infty}^{+\infty} s(t)^2 dt \int_{-\infty}^{+\infty} r(t)^2 dt}} \right| \quad (1)$$

Here in equation (1), $s(t)$ and $r(t)$ are the TX and RX signals, respectively. The highest value of cross-correlation among transmitting and receiving pulse-estimate the signal falsification known as fidelity factor. Typically, the pulse become almost unrecognizable if an alteration is higher than 50% ($FF < 0.5$) [20]. For face to face and side by side orientation, the fidelity factors are 82% and 90% which indicate that the proposed system has lower distortion of the signal while transmitting UWB impulse signals. A low-

variation transmission coefficient, constant group delay and a decent fidelity factor illustrate good phase linearity of the proposed antenna at desired UWB based Microwave Imaging system.

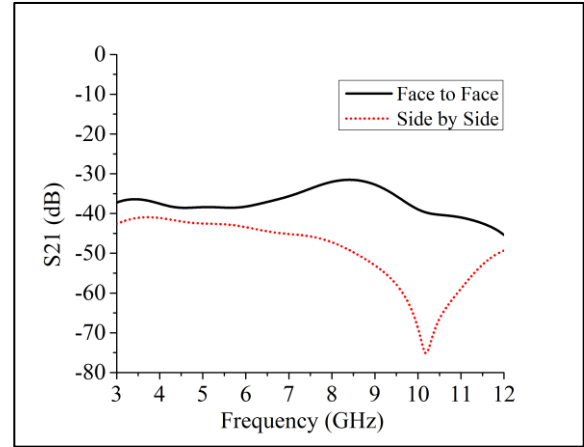


Fig. 14. Transmission coefficient in the face to face and side by side scenario

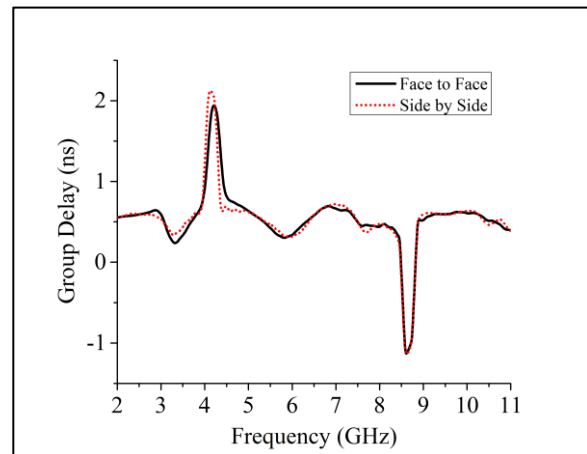
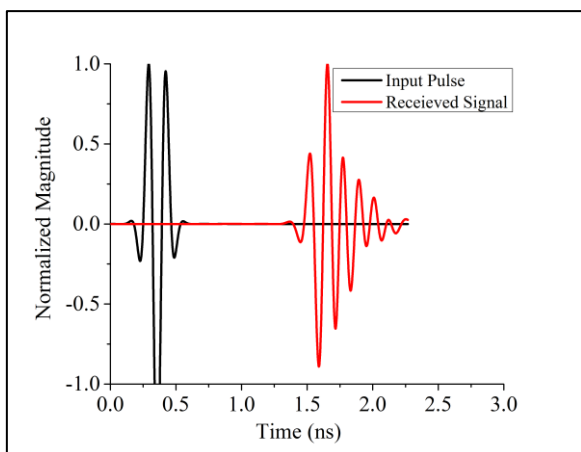
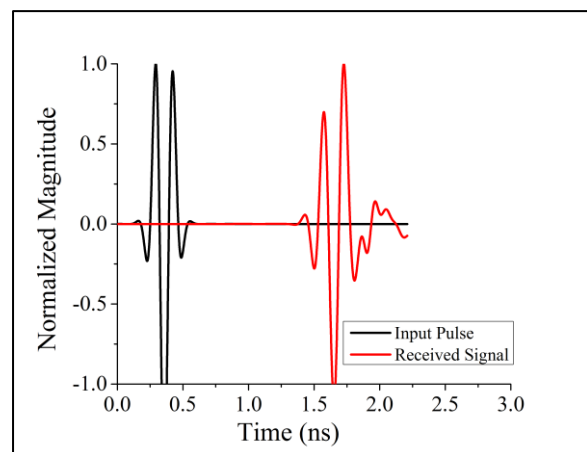


Fig. 15. Group Delay in face to face and side by side scenario



(a)



(b)

Fig. 16. Input and received pulse waveforms in (a) face-to-face and (b) side-by-side scenario

C. Microwave imaging setup and measurement

The system setup of anticipated antenna array for breast imaging is shown in Fig. 17. The main aim is to identify the change of backscattering signal with and without the present of tumor which has high dielectric inclusion. Similar breast phantom containing a tumor inside is used in the system which has high dielectric constant. The electrical properties of the breast phantom consist of two layers, breast tissue layer, and skin layers. The breast tissue stratum has a dielectric constant of 5.14 with 8.75 cm width and conductivity of 0.141 S/m. The skin layer is consisting of dielectric constant $\epsilon_r=38$ with 1.49 S/m conductivity which has 2.5 mm width. A tumor located 6 mm inside from the skin layer has a diameter of 10 mm containing higher dielectric constant of near 67. Generally, the tumor cell has higher dielectric constant comparing with normal breast tissue such as fat due to its high watery content.

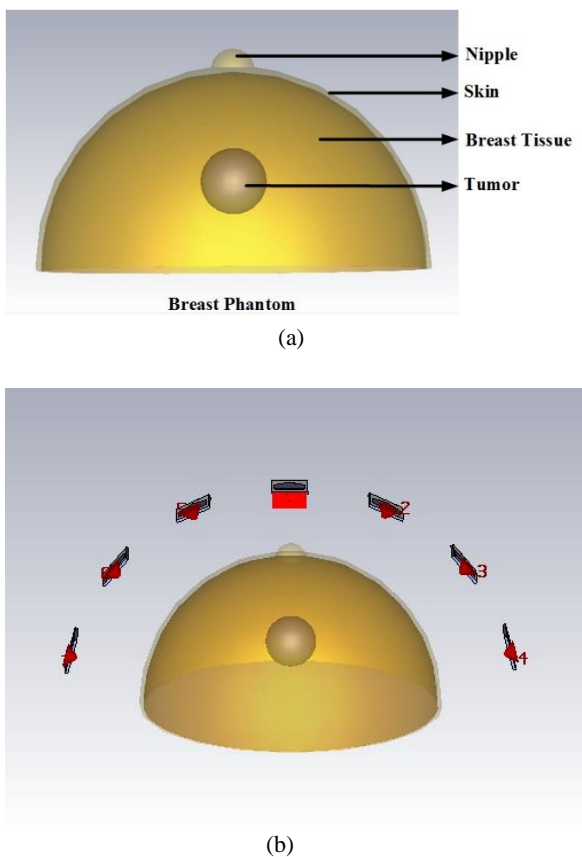
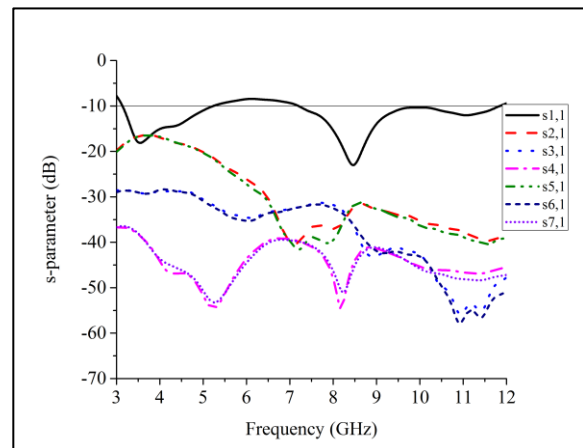


Fig. 17. Microwave imaging setup: (a) breast phantom and (b) antenna array setup surrounding phantom

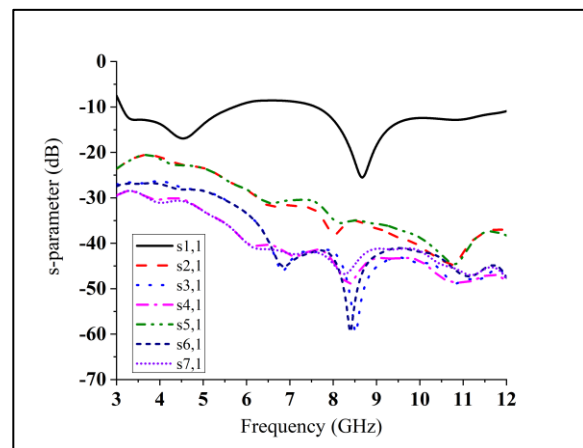
In order to observe the performance of the 7 antennas array system, the correlation among S_{11} , S_{21} , S_{31} , S_{41} , S_{51} , S_{61} , S_{71} is examined. The S-parameters are obtained by placing the antenna on the surrounding of breast phantom at a distance of 45 mm from the surface. The reflection coefficient is also noted with the antennas detached by 25 degrees. The antenna array works within 3 to 12 GHz. Fig.

18 displays the s-parameters of the antenna array system for two different setups of with and without tumor cell inside the phantom. A significant change in received signal is observed for these two scenarios.

Fig. 19 shows the simulated imaging results of the electric field of the array model for the breast tumor detection system. For two different frequencies of 3.5GHz and 6.5GHz, the backscattering signals are analyzed. It is seen that due to the different properties of the dielectric of tumor cell and breast tissue, tumor cell transmits more signal than normal breast tissue, as a result, the scattering percentage of the signals inside normal tissue is greater than tumor cell. So, the received signals density is high towards the tumor cell. So, the imaging results shows a significant difference among scattered signals of the tumor and normal breast tissue. So, the presence of tumor cell is identical. The portion of the existence of tumor cell is marked in Fig. 19.



(a)



(b)

Fig. 18. S-parameters of antenna array (a) with tumor and (b) without tumor

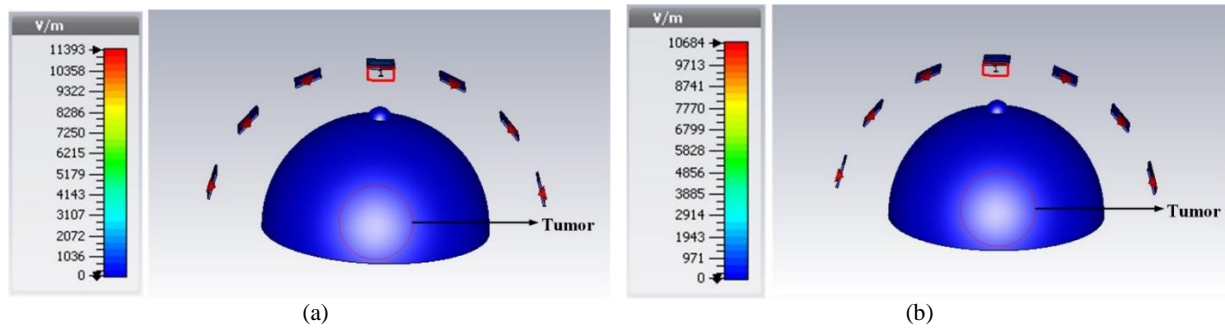


Fig. 19. Microwave Imaging results of the antenna array (a) 3.5GHz and (b) 6.5GHz

A comparative study between reported antennas with proposed one is listed in Table 2. The considered parameters are bandwidth, geometry antenna gain and

application. It is observed that the proposed antenna shows better performance than the reported antennas.

Table 2. Comparison between the reported antenna proposed antenna

Antennas	BW GHz (−10 dB)	Dimension Area (mm ²)	FB (%)	Gain (dBi)	Applications
[21]	3.80–11.85	30 × 30	102.00	not reported	Microwave Imaging
[19]	1.15–4.40	75 × 75	117.12	2.0–8.0	Microwave Imaging
[22]	4.00–9.00	30 × 30	76.92	2.0–6.0	Microwave Imaging
[23]	2.70–9.70	22.25 × 20	112.90	not reported	Microwave Sensing
Proposed	3.49 - 12	21.44 × 23.53	109.8	5.76	Microwave Imaging

4. Conclusion

The design and implementation of a compact wide slotted patch antenna having a dimension of 21.44 × 23.53 mm² are presented in this paper. An array of 7 antenna element surrounding a breast phantom is designed for screening. The simulated and experimental results analyzed to verify the performance of single antenna for UWB characteristics. The proposed antenna meets a good impedance matching, good gain, broader bandwidth with high efficiency and stable omnidirectional radiation patterns, which work within the bandwidth of 109.8% (3.49 – 12 GHz). The antenna shows good performance in both frequency domain and time domain scenario. The antenna array is used in breast phantom measurement system for locating tumor inside the breast. The variation of the antenna-backscattering signal for the presence of tumor inside the phantom made the array system an ideal candidate for microwave breast imaging.

Acknowledgements

This work was supported by the Ministry of Higher Education fundamental research grant FRGS/1/2018/TK04/UKM/01/3.

References

- [1] E. Fallenberg et al., *European Radiology* **24**(1), 256 (2014).
- [2] A. M. Hassan, M. El-Shenawee, *IEEE Reviews in Biomedical Engineering* **4**, 103 (2011).
- [3] E. C. Fear, P. M. Meaney, M. A. Stuchly, *IEEE Potentials* **22**(1), 12 (2003).
- [4] A. Shahzad, M. O'halloran, E. Jones, M. Glavin, *IEEE Antennas and Wireless Propagation Letters* **12**, 500 (2013).
- [5] M. Klemm, I. Craddock, J. Leendertz, A. Preece, and R. Benjamin, *International Journal of Antennas and Propagation* **2008**, pp. 1-9, (2008).
- [6] M. Z. Mahmud, M. T. Islam, M. N. Rahman, T. Alam, M. Samsuzzaman, *International Journal of Microwave and Wireless Technologies* **9**(10), 2013 (2017).
- [7] A. Afifi, A. Abdel-Rahman, A. Allam, A. A. El-Hameed, *Circuits and Systems (MWSCAS), 2016 IEEE 59th International Midwest Symposium on, 2016: IEEE*, pp. 1-4.
- [8] M. Mahmud, M. T. Islam, M. Samsuzzaman, S. Kibria, N. Misran, *IET Microwaves, Antennas & Propagation* **11**(6), 770 (2016).
- [9] N. R. Council, *National Academies Press*, 2001.

- [10] M. Lazebnik et al., *Physics in Medicine & Biology*, **52**(20), 6093 (2007).
- [11] T. Henriksson et al., *Antennas and Propagation Conference (LAPC)*, 2011 Loughborough, 2011: IEEE, pp. 1-4.
- [12] M. Klemm et al., in *Antennas and Propagation (EUCAP), Proceedings of the 5th European Conference on*, 2011: IEEE, pp. 3077-3079.
- [13] A. Modiri, S. Goudreau, A. Rahimi, K. Kiasaleh, *Medical Physics*, 2017.
- [14] R. Azim, M. T. Islam, N. Misran, *Arabian Journal for Science and Engineering* **38**(9), 2415 (2013).
- [15] R. Azim, A. Mobashsher, M. T. Islam, *Electronics Letters* **49**(15), 922 (2013).
- [16] R. Azim, M. T. Islam, N. Misran, A. T. Mobashsher, *Informacije MIDEM* **41**(1), 37 (2011).
- [17] R. Azim, M. T. Islam, N. Misran, *Telecommunication Systems* **52**(2), 1171 (2013).
- [18] R. Azim, M. T. Islam, N. Misran, *IEEE Antennas and Wireless Propagation Letters* **10**, 1190 (2011).
- [19] B. Wu, Y. Ji, G. Fang, *Electronic Measurement & Instruments*, 2009. ICEMI'09. 9th International Conference on, 2009: IEEE, pp. 2-226-2-229.
- [20] G. Quintero, J.-F. Zurcher, A. K. Skrivervik, *IEEE Transactions on Antennas and Propagation* **59**(7), 2502 (2011).
- [21] I. Hossain, S. Noghianian, S. Pistorius, *Antennas and Propagation Society International Symposium*, **2007** IEEE 5713 (2007).
- [22] S. Adnan, R. A. Abd-Alhameed, H. I. Hraga, I. T. Elfergani, J. M. Noras, R. A. Halliwell, 2011.
- [23] H. Kanj, M. Popovic, *IEEE Antennas and Wireless Propagation Letters* **4**(1), 397 (2005).

*Corresponding author: p94299@siswa.ukm.edu.my